Heat Dissipation Performance of Micro-channel Heat Sink with Various Protrusion Designs

Siyuan Bai [1], *Khalil Guy* [2], *Yuxiang Jia* [1], *Weiyi Li* [1], *Qingxia Li* [2], *Xinyao Yang* [1]

[1]Xi'an Jiaotong-Liverpool University, China
[2]Fisk University, USA

Siyuan.Bai17@student.xjtlu.edu.cn (S.B.); khalil.guy@my.fisk.edu (K.G.); Yuxiang.Jia17@student.xjtlu.edu.cn (Y.J.); Weiyi.Li16@student.xjtlu.edu.cn (W.L.);qli@fisk.edu (Q.L.); Xinyao.Yang@xjtlu.edu.cn (X.Y.)

Abstract

This research will focus on studying the effect of aperture size and shape of the micro-channel heat sink on heat dissipation performance for chip cooling. The micro-channel heat sink is considered to be a porous medium with fluid subject inter-facial convection. Derivation based on energy equation gives a set of governing partial differential equations describing the heat transfer through the micro-channels. Numerical simulation, including steady-state thermal analysis based on CFD software, is used to create a finite element solver to tackle the derived partial differential equations with properly defined boundary conditions related to temperature. After simulating three types of heat sinks with various protrusion designs including micro-channels fins, curly micro-channels fins, and Micro-pin fins, the result shows that the heat sink with the maximum contact area per unit volume will have the best heat dissipation performance, we will interpret the result by using the volume averaging theorem on the porous medium model of the heat sink.

Keywords: Porous medium model of heat sink; Volume averaging theorem; CFD simulation

Mathematics Subject Classification:

Introduction

1   Introduction

Driven by rapid development and performance boost of integrated circuit chips used in computers [3], the need for more efficient heat transfer performance has dramatically increased in recent decades. Indeed, the heat transfer method can be achieved by various approaches, including the application of interfacial convection of air and other coolant [13]. The heat sink is a widely used device in Electronic Packaging for heat transfer of heat-generating electronic components in electrical appliances. They are practically made of aluminum alloy, brass or bronze, into the shape of plates, sheets, and multiple sheets. The solid part is soldered to the electronic equipment, while the coolant fluid is flowing through the solid and drops the temperature by inter-facial convection. Usually, the heat sink shall be coated with a layer of heat-conducting silicon grease on the contact surface between the electronic components and the heat sink, so that the heat generated from the electronic components can be transferred to the heat sink more efficiently, then be distributed to the surrounding coolant fluid through the heat sink.

In a typical microchannel heat sink, the width of each micro-channel is usually small compared to the full scale of the entire heat sink, and the micro-channels fit tightly over the heat sink. Adjacent microchannels are separated by silicon

fins, allowing the coolant fluid to divert into different micro-channels. Various factors affect the performance of heat sink, such as convection velocity, the effective thermal conductivity of the material, and the protrusion design of the heat sink. Zhao and Lu [16] compared two analytical approaches: the porous medium model and the fin approach, they found that the analytical solution based on the porous medium approach agreed much more excellently with numerical calculations, while the fin approach overestimated the heat transfer due to the assumption that the fluid temperature in the direction perpendicular to the coolant flow is constant.

Previous empirical research has given proof and examples to the application of the porous medium method. The porous medium model is represented by a mixture of solid phase with a hollow skeleton and fluid flowing through the void. Khoei and Vahab considered the solid phase of the porous media as the main skeleton supporting basic geometric structure while the fluid phase flowing through the voids was defined as a filler [6]. The heat conduction behavior of the entire porous medium depends mostly on the interaction between solid skeleton and fluid phase. To further study the behavior of the porous media, they stated that the mixed structure of the porous media could be calculated appropriately using averaging theorem[15]. The method of volume averaging is a technique to derive continuum equations for multi-phase systems, while the direct analysis of the process of fluid transport through the small pores is usually difficult, if not impossible, because of the complex structure of the porous medium.

Other methods can also be used to estimate the performance of a heat sink, though under some specific constraints, see, e.g., [5], in which the heat sink thermal resistance model was built for the ducted flow, where the air is forced to flow through a microchannel over the heat sink. Moreover, experimental tests are one of the popular methods to determine heat sink thermal performance[9]. However, the results may be optimistic and misleading. Nevertheless, experiments can provide measurements for only some specific quantities, at a limited time instance, and can often become complicated and expensive for some operating conditions. In these circumstances, a theoretical model is usually used as a first estimate; then numerical method or Computational Fluid Dynamics (CFD) simulation software, such as Ansys CFX, can give the insight to flow or heat transfer phenomena, therefore provide a qualitative prediction before a physical model has been made.

In this paper, we will employ the porous medium model, investigate the heat transfer process by analyzing the governing energy equations, then study the factors that affect the heat transfer performance. Meanwhile, we will carry out experiments using CFD simulation to validate the analysis.

2   Porous Medium Model

In this section, we will briefly review the heat conduction theorem, and introduce the non-local thermal equilibrium model for the two-phase flow, then derive the governing differential equations for heat conduction processes in the micro-channel heat sink by using the method of volume averaging and analyze the key factors that affect the heat dissipation performance from the governing equations.

According to the first conservation law of energy thermodynamics, the change in energy of a system is equal to the difference between the net heat transferred to the system and the net work done by the system. To describe the physical meaning mathematically, we recall the governing energy equation for the fluid and solid phases is (see, e.g., [12]),

$$\rho C_p \frac{\partial T}{\partial t} = \nabla \cdot k \nabla T + \dot{q}, \tag{1}$$

where $\dot{q}$ is the rate at which energy is generated per unit volume of the medium, k is the thermal conductivity, ρ is

the density of the medium, and C_p is the specific heat at constant pressure. Equation (1) states that rate of increase of energy stored, which is closely related to the properties of the material of the heat sink itself such as density and specific heat, is equal to the sum of the net energy outflow rate and energy generation rate.

A simple form of the macroscopic equation for forced convection of incompressible flow in a porous medium was obtained by the volume averaging of the conservation equations of the solid and the fluid over a representative elementary volume (REV)[4], using the Local Thermal Equilibrium assumption that the difference between the local fluid and solid temperature is negligible throughout the representative elementary volume (REV) under consideration. The one-equation model is given as follows,

$$(\rho C_p)_m \frac{\partial \bar{T}}{\partial t} + \nabla \cdot [\mathbf{v}\bar{T}] = \alpha_f \left(\frac{k_m}{k_f} + \frac{k'}{k_f} \right) \nabla^2 \bar{T} + (1-\phi)q, \tag{2}$$

where $\bar{T}$ is the macroscopic variable given by volume averaging, α_f is the thermal diffusivity of the fluid, k_m is the effective thermal conductivity, k' is the thermal dispersion conductivity, k_f is the thermal conductivity of the fluid, ϕ is the porosity, and $\mathbf{v}$ is the Darcy velocity, note that in the equation, ρ is the average density of the mixed porous medium structure involves the density of solid and fluid,

$$\rho = \phi \rho_f + (1-\phi)\rho_s, \tag{3}$$

where ρ_s represents the density of solid and ρ_f represents the density of fluid.

The one-equation model can save the time of computation. However, the assumption that the temperature difference between fluid and solid is negligible may increase the inaccuracies of the energy estimate. For this reason, we will introduce the Non-local thermal equilibrium (NLTE) model. The energy equations representing the thermal characteristics are defined for solid and fluid respectively are given as,

$$(\rho C_p)_f \left[\frac{\partial T_f}{\partial t} + \nabla \cdot (\mathbf{v}_f T_f) \right] = \nabla \cdot (k_f \nabla T_f), \tag{4}$$

and

$$(\rho C_p)_s \frac{\partial T_s}{\partial t} = \nabla \cdot (k_s \nabla T_s) + q, \tag{5}$$

where q is a heat source associated with the solid phase (such as the heat generated by attached chip), and it is assumed that the temperature and heat flux are continuous between the solid and the fluid phases, that is,

$$T_f = T_s \quad \text{on} \quad A_{fs}, \tag{6}$$

and

$$\mathbf{n}_{fs} \cdot k_f \nabla T_f = \mathbf{n}_{fs} \cdot k_s \nabla T_s \quad on \quad A_{fs}, \tag{7}$$

where A_{fs} is the interface between two phases.

3   Volume Averaging Method

In this section, we will apply the method of volume averaging to equations (4) - (5), to derive a basic form of two-equation NLTE model of heat transfer in heat sinks.

The method of volume averaging was developed by Slattery [10] and Whitaker [14], it relates the average of a gradient to the gradient of an average, therefore the macroscopic governing equations can be derived from the microscopic equations in porous media.

Considering a REV consists of both solid and fluid phases, the phase average of a quantity ε is defined as:

$$\langle \varepsilon \rangle = \frac{1}{V} \int_V \varepsilon \mathrm{d}V \tag{8}$$

where V is the total of volume V_f of the fluid phase and volume V_s of the solid phase. We also introduce the intrinsic phase average of a quality (see, e.g., [7]), which is defined as:

$$\bar{\varepsilon}_\alpha = \frac{1}{V_\alpha} \int_{V_\alpha} \varepsilon_\alpha \mathrm{d}V, \tag{9}$$

where ε_α is a physical quantity only in α-phase (α could be either solid or fluid). Since ε_α is considered to be zero in phases other than its intrinsic phase, equation (9) can be rewritten as:

$$\bar{\varepsilon}_\alpha = \frac{1}{V_\alpha} \int_V \varepsilon_\alpha \mathrm{d}V, \tag{10}$$

consequently, we obtain that

$$\langle \varepsilon_\alpha \rangle = \varphi_\alpha \bar{\varepsilon}_\alpha \tag{11}$$

where $\varphi_\alpha = \frac{V_\alpha}{V}$ is the volume ratio of α-phase in the porous medium. Moreover, in the porous medium model,

$$\langle \varepsilon_f \rangle = \phi \bar{\varepsilon}_f \quad and \ \langle \varepsilon_s \rangle = (1 - \phi)\bar{\varepsilon}_s. \tag{12}$$

Lemma [Volume Averaging Theorem]

$$\frac{1}{V} \int_{V_\alpha} \nabla \varepsilon_\alpha dV = \nabla \left[\frac{1}{V} \int_{V_\alpha} \varepsilon_\alpha \mathrm{d}V \right] + \frac{1}{V} \int_{A_{\alpha\beta}} \varepsilon_\alpha \mathbf{n}_{\alpha\beta} \mathrm{d}S, \tag{13}$$

and

$$\frac{1}{V} \int_{V_\alpha} \nabla \cdot \varepsilon_\alpha \mathrm{d}V = \nabla \cdot \left[\frac{1}{V} \int_{V_\alpha} \varepsilon_\alpha \mathrm{d}V \right] + \frac{1}{V} \int_{A_{\alpha\beta}} \varepsilon_\alpha \cdot \mathbf{n}_{\alpha\beta} \mathrm{d}S, \tag{14}$$

where $A_{\alpha\beta}$ is the interface between two phases contained in the REV, and $\mathbf{n}_{\alpha\beta}$ is the normal vector to the interface.

Integrating equations (4) and (5) with respect to the REV and dividing the resulting expression by V, we note that $\mathbf{v}_f \cdot \mathbf{n}_{fs} = 0$ by assuming the solid is rigid and impermeable,

$$\frac{\partial}{\partial t}\left[\phi\left(\rho C_p\right)_f \bar{T}_f\right] + \left(\rho C_p\right)_{\mathrm{f}} \nabla \cdot \left[\phi \overline{\mathbf{v}_f T_f}\right] = \nabla \cdot \left[k_{\mathrm{f}} \nabla \rho \bar{T}_f\right] + \nabla \cdot \left[\frac{1}{V}\int_{A_{fs}} k_{\mathrm{f}} T_{\mathrm{f}} \mathbf{n}_{fs}\mathrm{d}S\right]$$
$$+ \frac{1}{V}\int_{A_{fs}} k_{\mathrm{f}} \nabla T_{\mathrm{f}} \cdot \mathbf{n}_{fs}\mathrm{d}S,$$

and

$$\frac{\partial}{\partial t}\left[(1-\phi)\left(\rho C_p\right)_s \bar{T}_s\right] = \nabla \cdot \left[k_s \nabla(1-\phi)\bar{T}_s\right] - \nabla \cdot \left[\frac{1}{V}\int_{A_{fs}} k_s T_s \mathbf{n}_{fs}dS\right] - \frac{1}{V}\int_{A_{fs}} k_s \nabla T_s \cdot \mathbf{n}_{fs}\mathrm{d}S + q,$$

Then the two-equation model can be written as:

$$\begin{cases} \phi\left(\rho C_p\right)_f \left[\frac{\partial}{\partial t}\bar{T}_f + \nabla \cdot \left(\overline{\mathbf{v}_f T_f}\right)\right] = \phi \nabla \cdot \left[\left(k_f + k'\right)\nabla \bar{T}_f\right] + q_{sf}, \\ (1-\phi)\left(\rho C_p\right)_s \frac{\partial}{\partial t}\bar{T}_s = (1-\phi)\nabla \cdot \left(k_s \nabla \bar{T}_s\right) - q_{sf} + q, \end{cases}$$

where q_{sf} can be interpreted as the heat flux from the solid phase to the fluid phase per unit volume, it can be expressed as [11]:

$$q_{sf} = \frac{A_{sf}h_{sf}\left(\bar{T}_s - \bar{T}_f\right)}{\frac{V_s}{(1-\phi)}} = h_{sf}\left(\bar{T}_s - \bar{T}_f\right)ss = (1-\phi)\eta\frac{1}{d}h_{sf}\left(\bar{T}_s - \bar{T}_f\right), \tag{15}$$

where d is the microscopic length scale, and $\eta = \frac{A_{fs}d}{V_s}$ represents the distribution of the solid.

The above equations provide a theoretical basis of the fact that the heat dissipation effect is closely related to the protrusion design of the micro-channel heat sink, we conclude from the model that the heat dissipation performance will be improved by, of course, increasing the contact area per unit volume, but also reducing the microscopic length of the pores, for example, one can design smaller path scale or more paths in a REV to improve the heat dissipation performance.

CFD software experiments

In this section, we will describe the experiments that we have simulated using CFD software. We tested the three protrusion designs of the heat sink, where the fins were in regular shape, wave shape, and needle shape, respectively. See Figure 1-3:
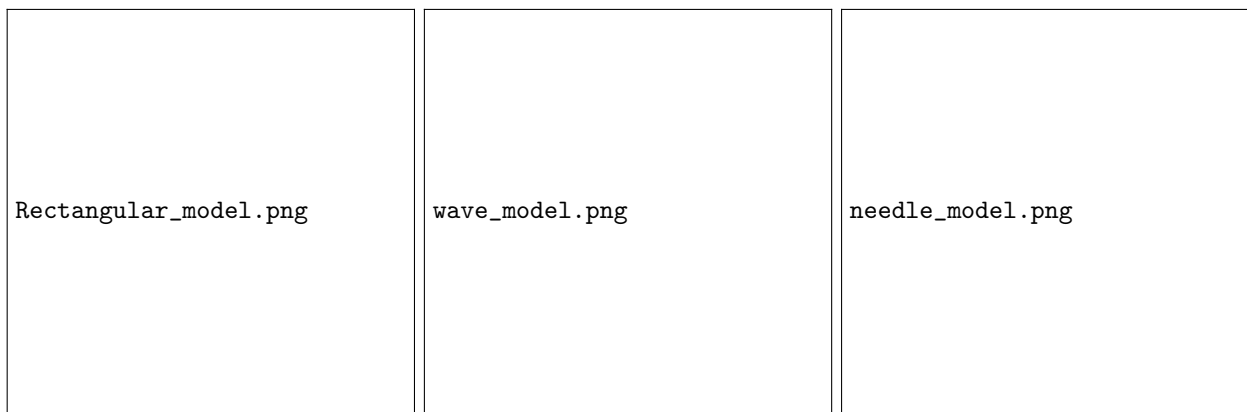
The heat sink with regular shape has 14 active and visible bodies, including 13 fins and one base, together with 12 cooling microchannels. The fins and base are made by structural steel with all the properties of this material preassumed. All 26 bodies have been meshed, participated in the simulation to reflect the heat dissipation effect
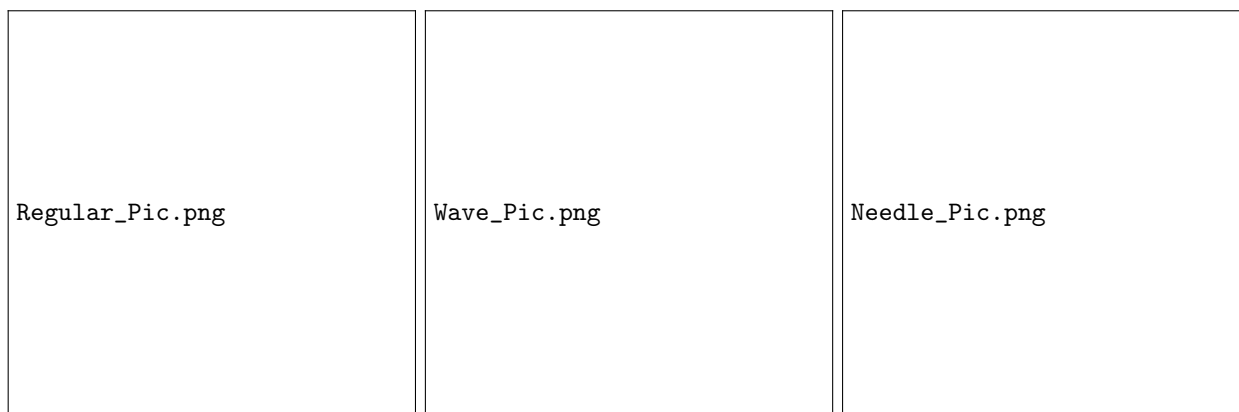
Figure 1: Regular   Figure 2: Wave   Figure 3: Needle

through the value of the steady-state temperature. In the experiments, we let the surrounding air temperature be $22°C$ and use it to be the cooling fluid. See the configuration in Figure 1:

Table 1: **The configuration of the experiments**

Dimensions/Materials	
Dimension of the base-plate	10 mm × 10 mm × 0.4 mm
Height of the fins/pins	24 mm
Materials	Structural Steel
Cooling fluid	Air
Initial Temperature	$22°C$
Heat source temperature	$55°C$
Convection coefficient	$200W/(m^2 \cdot ° C)$
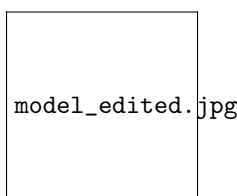
At the beginning of each experiment, the temperature of the model is the same as the surrounding temperature, which is $22°C$. Soon after, the CPU starts to run (introduced as a heat source attached to the bottom of the base plate). We set the temperature of the heat source to be $55°C$, which is the normal temperature of most CPU when they are running basic programs. We assume that the heat generated by the CPU is transferred to the heat sink evenly and continuously. Simultaneously, the coolant air passes through the microchannels. We set the convection coefficient to be $200W/(m^2 \cdot ° C)$ as in Table 1. The thermal steady result of the regular-shaped heat sink is given in Figure 4:

To analyze the heat dissipation effect, we built control groups for a large number of experiments. First, we conducted a set of controlled trials by changing the number of fins on the base plate to increase the contact surface area per unit volume. The results are provided in Table 2:

Next, we decrease the path size of the fins and set up control groups to conduct experiments. The result is illustrated in Table 3:
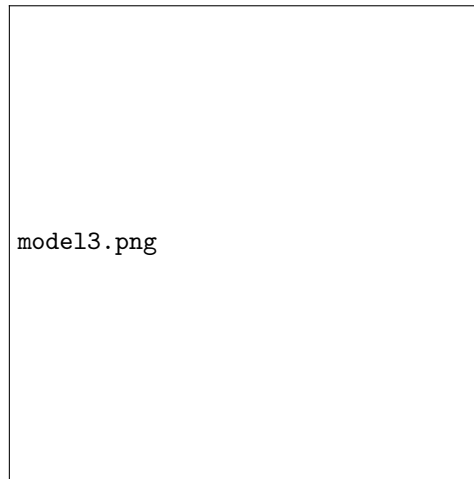
Figure 4: Thermal Steady Result of regular-shaped heat sink

Table 2:

Number of Fins	Maximum Temperature
4	$54.730°C$
8	$54.717°C$
13	$54.716°C$

4   Discussion

In the experiment, we compared heat sinks with three different protrusion designs: the regular shape, the wave shape, and the needle shape. The performance was assessed according to the minimum temperature over the heat sink.

In simulating the regular-shaped heat sink, we conducted four experiments with the width of the channel as an independent variable. For the value of each micro-channel width, we took the number of fins as an independent variable and carried out three sub-experiments respectively. The result temperature obtained after 2 seconds are displayed in Table 4: Since all the maximum temperatures occur on the base where the chip is attached, and all the minimum temperatures occur on the cooling fins, a lower maximum temperature indicates a better performance of the heat sink. Therefore, we see that with the fixed size of the base, increasing the number of fins and reducing the channel width both result in a larger specific area per unit volume of the heat sink, see Figure 5:

In regular-shaped heat sink, the difference between heat dissipation performances is subtle when we compared heat sinks with same numbers of fins but different path sizes. However, this causes a defect of the experiment design so the data could be misleading. The heat sink is not fully covered by the cooling fins when we set the path width as $200\mu m$ or $100\mu m$. Therefore, the convection over the base plate is enhanced so that a lower maximum temperature could be reached. To further validate the conclusion from the model, we simulated two other protrusion designs of the heat sink: wave-shaped and needle-shaped. The results are demonstrated in Figure 6 and Table 5:

Among the three experiments, the needle-shaped heat sink displayed the best heat dissipation performance, by reaching $52.261°C$ in minimum temperature. The result of this comparison is consistent with the analytical result based on the NLTE model, that is, for the heat sink made by a particular material, the heat dissipation performance can be improved by a better protrusion design, including the increase of the contact surface per unit volume and the reduction

Table 3:

Fin Spacings (μm)	Maximum Temperature ($^\circ C$)
400	54.716
300	54.700
200	54.676
100	54.692

Table 4: **Heat dissipation performance of regular-shaped heat sink**

Model	Channel Width(μm)	No. of Fins	Initial Temp.($^\circ C$)	Max. Temp.($^\circ C$)	Min. Temp.($^\circ C$)
1	400	4	55	54.730	53.170
2	400	8	55	54.717	53.170
3	400	13	55	54.716	53.170
4	300	4	55	54.712	53.158
5	300	8	55	54.727	53.158
6	300	13	55	54.700	53.158
7	200	4	55	54.717	53.140
8	200	8	55	54.721	53.140
9	200	13	55	54.676	53.140
10	100	4	55	54.684	53.105
11	100	8	55	54.692	53.105
12	100	13	55	54.692	53.105

of the microscopic length scale.

5   Conclusion

Based on the porous media model constructed by a mixture of fluid and solid phase, we derived the two-equation non-local thermal equilibrium model using the method of volume averaging; then, we analyzed the factors that affect heat dissipation performance from the energy equations. The heat dissipation capability of the heat sink performs better with greater contact surface area per unit volume and appropriate protrusion design, which provides smaller microscopic length.

Heat sinks with three different geometries: regular-shaped heat sink, wave-shaped heat sink, and needle-shaped heat sink are tested by using CFD steady-state analysis. After comparing the heat dissipation performance demonstrated by the minimum temperature that the heat sinks dropped to, it is found that the micro-channel heat sink with needle pins gives the best heat dissipation performance, according to the measured temperature drop. For the regular-shaped heat sink, the better heat dissipation effect can be achieved by adding contact surface area; the wave-shaped heat sink has a relatively better performance on heat dissipation because of the greater contact area, but the improvement is limited because the microscopic length is not reduced; the needle-shaped heat sink displays the best heat dissipation performance among the three tests due to the greater contact surface area per unit volume and smaller microscopic length.

As ongoing research in material sciences enables the optimization of related conditions such as heat transfer coefficient
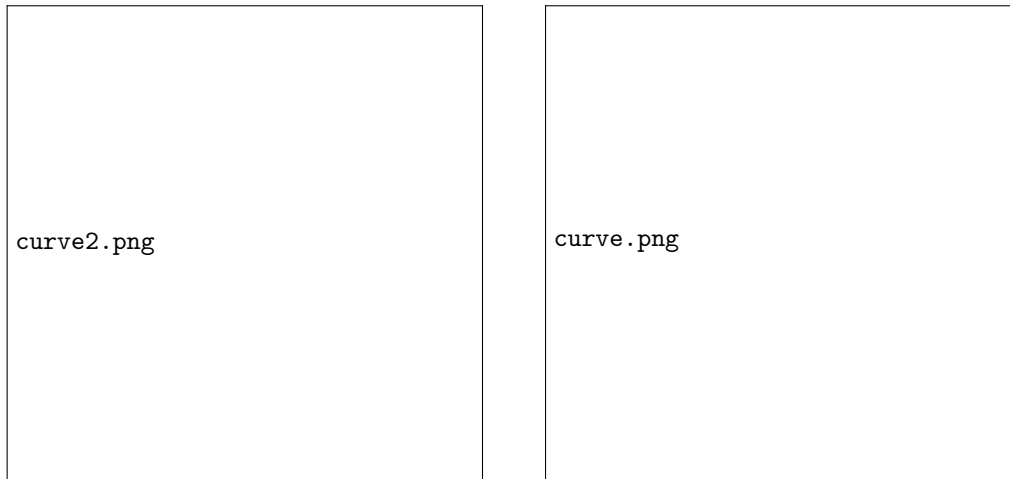
Figure 5: Characteristic curves of Heat Dissipation Performance
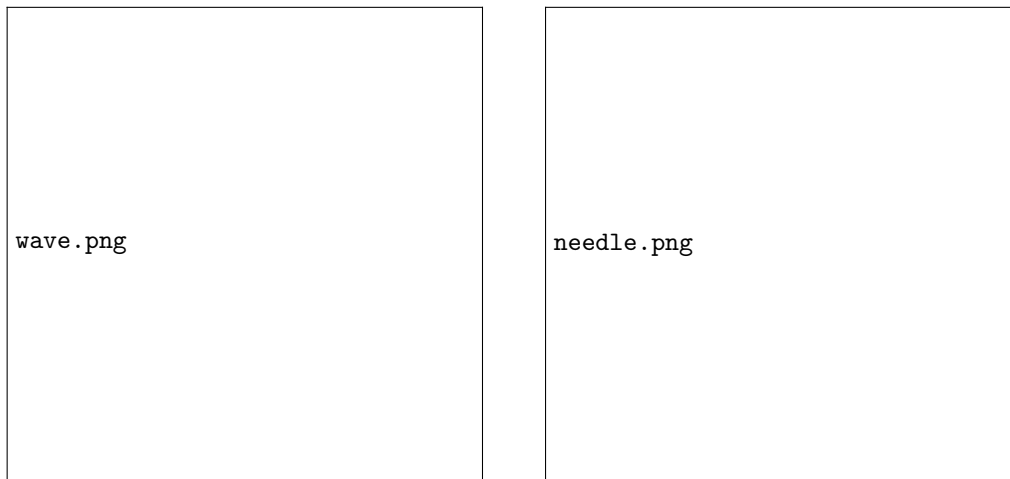

Figure 6: Thermal Steady Result of Wave-shaped and Needle-shaped Heatsinks

and specific heat of the materials, and the rapid-developed micro-manufacturing creates the possibility for the production of more delicate components, more attention could be given to the improvement of the protrusion design for the heat sink, such as combining micro-channels and micro-heat pipes[2]. Further study in this topic could be carried out on determining the optimal porosity. Besides, it is possible to consider the coupling of continuity equation and momentum equations to complete the porous medium model; also, the characteristics of the new heat sink models, such as flared fins, could be studied.

Conflict of Interest

The authors declare no conflict of interest.

Funding Statement

Table 5: **Thermal Steady Result of the three controlled experiments**

Fin Shape	Regular	Wave	Needle
Minimum Temperature Reached	$53.17^\circ C$	$53.144^\circ C$	$52.261^\circ C$

References

[1] Bergman, T. L., Lavine, A. S., Incropera, F. P. and Dewitt, D.P., *Fundamentals of Heat and Mass Transfer.*; Wiley: Hoboken, 2011.

[2] Principles and prospects of micro heat pipes, in *Proc. 5th Int. Heat Pipe Conf.*, Tsukuba, Japan, pp. 325 – 328.

[3] Geer, D., Chip makers turn to multicore processors. *IEEE* **2005**, *38(5)*, 11–13.

[4] Hsu, C.T., Cheng, P., Thermal dispersion in a porous medium. Int J Heat Mass Transf **1990**, *33*,1587–1597.

[5] Jeggels, Y. U., Dobson, R. T. and Jeggels, D. H., Comparison of the cooling performance between heat pipes and aluminium conductors for electronic equipment enclosures, *Proceedings of the 14th International Heat Pipe Conference*, Florianópolis, Brazil.

[6] Khoei, A. R. and Vahab, M., *A numerical contact algorithm in saturated porous media with the extended finite element method*, Comput. Mech., 2014.

[7] Liu, W., Fan, A. and Huang, X., *Theory and Application of Heat and Mass Transfer in Porous Media*; Sciencep: Beijing, China, 2006.

[8] Nield, D. A. and Bejan, A., *Convection in Porous Media*; Cham: Springer, 2017.

[9] Sergent, J. E. and Krum, A., *Thermal management handbook: for electronic assemblies*; McGraw Hill Professional, 1998.

[10] Slattery, J. C., Flow of viscoelastic fluids through porous media. *AIChE Journal* **1967**, *13(6)*, 1066–1071.

[11] Su, Y. and Davidson, J. H., *Modeling Approaches to Natural Convections in Porous Media*; Cham: Springer, 2015.

[12] Welty, J. R., Wicks, C. E., Wilson, R. E. and Rorrer G. L., *Fundamentals of Momentum, Heat and Mass Transfer*; Wiley: Hoboken, 2008.

[13] Willingham, T. C. and Mudawar, I., Forced-convection boiling and critical heat flux from a linear array of discrete heat sources, *Int. J. Heat Transfer* **1992**, *35(11)*, 2879–2890.

[14] Whitaker, S., Diffusion and dispersion in porous media. *AIChE Journal* **1967**, *13(3)*, 420–427.

[15] Whitaker, S.; *The method of volume averaging* (Vol. 13); Springer Science Business Media: Dordrecht, 1999.

[16] Zhao, C. Y. and Lu, T. J., Analysis of microchannel heat sinks for electronics cooling, *Int. J Heat and Mass Transfer* **2002**, *45*, 4857–4869.